

Compressibility of porous metals in shock waves

R. F. Trunin, G. V. Simakov, Yu. N. Sutulov, A. B. Medvedev, B. D. Rogozkin,
and Yu. E. Fedorov

(Submitted 23 January 1989; resubmitted 4 April 1989)
Zh. Eksp. Teor. Fiz. **96**, 1024–1038 (September 1989)

New data on the compressibility of porous chromium, tantalum, magnesium, and cobalt samples are obtained in shock-wave experiments. Additional results are also obtained for heretofore unstudied states of copper, iron, nickel, molybdenum, and lead. An equation of state is chosen to describe the aggregate of the experimental results.

INTRODUCTION

No new studies of the dynamic compressibility of metals having a low initial density have been published for the region of states investigated in Refs. 1 and 2. The subsequently obtained experimental data pertained either to much higher energy states³ or to relatively narrow range near the shock adiabat of a solid metal.⁴ No experiments were performed at pressures and densities that are relatively high but are substantially lower than crystallographic. In the only existing publications⁴ are reported the first measurements at pressures $P < 5$ GPa, where a shock adiabat of one form or another is "formed." Furthermore, the assortment of metals investigated in Refs. 1, 2, 4, and 5 was small, and more precise measurements were needed in a number of cases.

All the above has stimulated the present investigation. We report here the measured compressibilities of porous chromium, tantalum, magnesium, and cobalt, and present for copper, iron, nickel, molybdenum, tungsten, and lead additional data pertaining mainly to the uninvestigated region of states.

EXPERIMENTAL RESULTS

The samples (as a rule cylindrical washers 12–15 mm in diameter and 1.5–5.0 mm thick) were made by pressing the powdered metals to the required initial density $\rho_{00} = \rho_{0,cr} / m$ ($\rho_{0,cr}$ is the crystallographic density of the metal and m is the porosity). The lowest density (maximum porosity) was reached by sublimating a light organic component mixed with a fine-grained ground powder of the metal. The powder brands, the contents of the main elements, and the ranges of particle dimensions are listed in Table I.

The compression parameters were determined by a reflection method.⁶ A relatively large variation of the compression parameters of the investigated metals was obtained by a set of measuring blasting systems based for the most part on acceleration of metallic striker plates by the blast products. Their velocities ranged from 0.3 to 9 km/s. An electric-contact method was used to measure the wave velocities.⁶ When the pressure in the samples were lower than 5 GPa, the time markers were as a rule piezoceramic sensors. Calibration experiments were performed to assess the influence of various factors on the recorded shock-wave velocities.

We varied in these experiments the dimensions of the individual powder particles, the sample humidity, and the sample thickness. We monitored in addition the effect of the air filling the pores between the individual powder particles. These measurements were performed as a rule at pressures

$P > 5$ GPa. The various ranges were: particle sizes—from a few to several times ten microns; humidity—from that of the ambient to near zero (thoroughly dried powders); the samples differed in thickness by an approximate factor 2–3 (1.5–5 mm). In Ref. 7 were performed two sets of experiments on copper powders, with the sample thicknesses (80 mm) exceeding by more than an order the customary standard dimensions. Experiments with evacuated samples (normal filling density, pressure of order of several Torr in the samples) were performed on copper.

It was shown in all cases that the foregoing factors has no noticeable effect whatever on the measured shock-wave velocities. This gave ground for assuming that the conditions of the shock waves compressing the porous samples in the investigated range of states were close to equilibrium. The experiments could therefore be standardized and the interpretation of the results significantly simplified.

All the experimental results are summarized in Tables II–VIII and plotted in the figures. These tables and figures show the averaged measurement results of both the principal and procedural experiments (since their results are equal within the limits of the experimental accuracy). Table IX shows data for nickel¹ reduced by the method of Ref. 7.¹⁾

Each wave velocity is here the result of several independent measurements with a particular blast device. As a rule the rms error of the wave velocity D in each run of experiments (each experimental point) does not exceed $\Delta D / D$ (1.0–2.0%). This estimate holds also for the error of $\Delta U / U$, where U and ΔU are the mass velocity behind the shock wave and its variation.

Figure 1 shows the data for the molybdenum; these are the so-called "single-charge lines," or plots that yield the adiabat of any porosity in the experimentally investigated Δm interval. Similar plots (see Tables II–VIII) can be drawn for most other investigated metals. It is of interest that starting with a certain m (in this case, with $m = 2.0$ – 2.5), for identical screen materials (aluminum in most experiments) and with identical states in them, the wave velocities in the porous samples do not depend on the initial sample density. This makes possible estimates of the adiabat positions also for m larger than in experiment, by using a small linear interpolation of the $D(m)$ plots. The gradient $\Delta D / \Delta m$ of the velocity decrease from the value $D(\rho_{0,cr})$ to the linear section (at $m \geq 2$ – 3) depends on the shock-wave intensity in the screen and is larger the lower this intensity.

The next three diagrams (Figs. 2–4) show the aggregate of the experimental data, plotted in the kinematic variables D and U , for copper, nickel, and molybdenum, which were investigated most thoroughly.²⁾ The observed peculiarities in the positions of the adiabats in these figures are com-

TABLE I.

Metal	Co	Mo	Pb	Cr	Fe	Cu	Ni	W	Mg	Ta
Powder brand	PK-1	MP-4	SO	PKh1S	PZh-1	PM-2	PNK	PVV	MPF	TKP
Main-element content, %	99.40	99.98	99.50	99.40	98.70	99.70	99.85	99.83	99.50	99.00
Particle dimensions, μm	>70-0.5%; >45-44.5%; <45-54.9%	<40	<20	<50	50-150; <100	~5	<10	<50	<60	5-65

mon, to one degree or another, also to adiabats of the other investigated metals. In addition to the new data, Figs. 2-4 show the results of Refs. 4, 5, and 7. On the whole, all the results are in satisfactory agreement, although the positions of some experimental points deviate from the general dependences determined by the aggregate of the data.

An analysis of the $D-U$ diagrams leads to a number of conclusions:

1. In those cases when the initial sections of the porous-metal adiabats were investigated in sufficient detail and in a wide range of m (for Cu, Mo, Ni—see Figs. 2-4), the plots form a fan of diverging straight lines tending to a small region ΔD_0 ($U=0$) adjacent to the origin.

2. The largest initial slopes D'_u are those of adiabats corresponding to small porosities; the adiabat slope decreases with increase of m . The slope changes also when the

wave velocities (on the considered adiabat) increase. The largest change takes place also for adiabats corresponding to small porosities.

3. For the metals listed in Sec. 1, the position of the adiabat for the maximum or near-maximum porosity is such that its linear extrapolation from large D and U to $U=0$ leads formally to negative D_0 and consequently, for certain $U < U_{cr}$, to negative wave velocities. This contradicts the conservation law, since $D > U$ is a mandatory condition for the existence of a shock wave. Investigation of these adiabats in the maximum slope region ($D=U$) has shown that the $D(U)$ dependence is convex here in a direction opposite to that of the small-porosity adiabats.

4. It follows from the general arrangement of the $D(U)$ plots that when the shock-wave intensities are increased the slopes of the porous-metal adiabats tend to the correspond-

TABLE II.

Molybdenum; $\rho_0=10.20 \text{ g/cm}^3$							
$D, \text{ km/s}$	$U, \text{ km/s}$	$P, \text{ GPa}$	$\rho, \text{ g/cm}^3$	$D, \text{ km/s}$	$U, \text{ km/s}$	$P, \text{ GPa}$	$\rho, \text{ g/cm}^3$
$\rho_{00}=8.12 \text{ g/cm}^3; m=1.26$				$\rho_{00}=5.59 \text{ g/cm}^3; m=1.82$			
2.26	0.47	8.7	10.26	0.835	0.30	1.4	8.72
2.79	0.67	15.2	10.68	1.29	0.585	4.2	10.23
3.48	0.92	26.1	11.05	1.95	0.92	10.0	10.58
4.10	1.13	37.8	11.23	2.66	1.25	18.5	10.56
4.89	1.50	59.3	11.71	3.27	1.52	27.8	10.45
5.75	1.98	92.4	12.38	4.10	1.97	45.1	10.76
6.22	2.09	106.0	12.23	4.71	2.30	60.8	10.96
6.58	2.36	126.0	12.66	5.15	2.51	72.3	10.90
6.97	2.60	147.0	12.95	5.54	2.66	82.5	10.77
				6.00	2.98	99.9	11.06
				6.58	3.31	122.0	11.25
				8.47	4.25	201.0	11.22
				10.08	5.25	296.0	11.67
$\rho_{00}=2.914 \text{ g/cm}^3; m=3.5$				$\rho_{00}=4.435 \text{ g/cm}^3; m=2.3$			
0.96	0.65	1.8	8.98	1.11	0.62	3.0	9.97
1.65	1.17	5.6	10.04	2.46	1.41	15.3	10.39
2.30	1.62	11.0	9.86	3.03	1.71	23.0	10.18
2.86	1.99	16.6	9.58	3.86	2.22	38.0	10.44
3.75	2.59	28.3	9.42	4.96	2.81	61.8	10.23
4.87	3.29	46.7	8.98	5.80	3.33	85.7	10.41
5.24	3.51	53.6	8.83	6.46	3.68	105.0	10.30
5.81	3.88	65.7	8.77	9.84	5.66	247.0	10.44
6.49	4.29	81.2	8.60				
9.57	6.30	176.0	8.53				
$\rho_{00}=2.55 \text{ g/cm}^3; m=4.0$				$\rho_{00}=1.72 \text{ g/cm}^3; m=5.93$			
0.972	0.654	1.6	7.63	3.82	3.02	19.8	8.21
1.628	1.207	5.0	9.86	4.97	3.81	32.6	7.37
2.30	1.68	9.8	9.46	5.35	4.07	37.5	7.19
3.80	2.68	26.0	8.65	6.61	5.01	57.0	7.11
4.01	2.84	29.0	8.74				
4.85	3.43	42.4	8.71				
5.25	3.66	49.0	8.42				
5.85	4.04	60.3	8.24				
6.41	4.40	71.9	8.13				
9.50	6.51	158.0	8.10				
				0.898	0.678	0.8	5.21
				1.574	1.35	2.7	8.98
				2.33	1.91	5.7	7.08
				2.95	2.39	9.0	6.67
				5.05	4.05	26.1	6.44

TABLE III.

Copper; $\rho_0=8.93 \text{ g/cm}^3$							
D, km/s	U, km/s	P, GPa	ρ , g/cm ³	D, km/s	U, km/s	P, GPa	ρ , g/cm ³
$\rho_{00}=6.33 \text{ g/cm}^3$; $m=1.41$				$\rho_{00}=4.465 \text{ g/cm}^3$; $m=2.0$			
1.828	0.534	6.2	8.94	0.713	0.315	1.0	8.00
4.58	1.77	51.3	10.32	1.26	0.606	3.4	8.60
6.90	3.06	134.0	11.37	1.97	0.996	8.8	9.03
10.03	5.06	321.0	12.77	2.69	1.35	16.4	8.96
$\rho_{00}=3.57 \text{ g/cm}^3$; $m=2.5$				$\rho_{00}=2.551 \text{ g/cm}^3$; $m=3.5$			
1.116	0.63	2.5	8.20	3.12	1.55	21.6	9.00
1.83	1.09	7.1	8.83	3.31	1.65	24.4	8.92
4.41	2.62	41.2	8.79	3.64	1.84	29.9	9.03
5.11	3.02	55.1	8.73	4.19	2.14	40.0	9.13
6.00	3.57	76.5	8.82	4.70	2.45	51.4	9.33
6.68	3.96	94.5	8.77	5.23	2.75	64.2	9.42
$\rho_{00}=2.977 \text{ g/cm}^3$; $m=3.0$				$\rho_{00}=1.639 \text{ g/cm}^3$; $m=5.45$			
1.73	1.15	6.0	8.91	5.07	3.39	43.8	7.70
2.40	1.595	11.4	8.88	5.50	3.61	50.7	7.72
2.86	1.83	15.6	8.26	5.98	4.01	62.0	7.74
3.41	2.23	22.6	8.60	6.74	4.43	76.1	7.44
3.92	2.53	29.6	8.42	$\rho_{00}=1.24 \text{ g/cm}^3$; $m=7.2$			
4.19	2.74	34.2	8.60	2.45	1.90	5.8	5.55
5.07	3.23	48.7	8.20	2.98	2.39	8.8	6.26
5.64	3.64	61.5	8.46	5.25	4.05	26.3	5.40
6.04	3.80	68.3	8.03	7.09	5.31	46.7	4.94
6.61	4.23	83.2	8.27	$\rho_{00}=2.232 \text{ g/cm}^3$; $m=4.0$			
9.57	6.29	179.0	8.69	0.946	0.661	1.4	7.41
$\rho_{00}=2.232 \text{ g/cm}^3$; $m=4.0$				1.66	1.235	4.6	8.72
2.33	1.725	9.0	8.58	2.93	2.12	14.0	8.17
4.07	2.89	26.2	7.70	4.77	3.51	40.0	7.16
5.10	3.51	40.0	7.16	5.41	3.77	45.5	7.36
5.41	3.77	45.5	7.36	6.07	4.16	56.4	7.09
6.07	4.16	56.4	7.09	6.81	4.61	70.1	6.91
6.81	4.61	70.1	6.91	9.51	6.68	142.0	7.50
9.51	6.68	142.0	7.50	$\rho_{00}=2.232 \text{ g/cm}^3$; $m=4.0$			

TABLE IV.

Cobalt; $\rho_0=8.80 \text{ g/cm}^3$							
D, km/s	U, km/s	P, GPa	ρ , g/cm ³	D, km/s	U, km/s	P, GPa	ρ , g/cm ³
$\rho_{00}=5.533 \text{ g/cm}^3$; $m=1.59$				$\rho_{00}=2.594 \text{ g/cm}^3$; $m=3.39$			
1.027	0.293	1.7	7.74	1.026	0.651	1.7	7.09
1.560	0.567	4.9	8.69	1.801	1.180	5.5	7.52
2.27	0.88	11.0	9.04	2.43	1.65	10.4	8.08
2.97	1.20	19.7	9.28	3.04	2.03	16.0	7.81
3.63	1.46	29.3	9.26	3.96	2.63	27.1	7.72
4.49	1.90	47.2	9.59	4.28	2.80	31.1	7.50
5.18	2.25	64.5	9.78	5.20	3.35	45.1	7.29
5.58	2.44	75.2	9.83	5.59	3.57	51.8	7.18
5.94	2.61	85.8	9.87	6.26	3.94	63.9	7.00
6.47	2.89	103.0	10.00	6.80	4.39	77.4	7.32
7.05	3.23	126.0	10.21	10.16	6.39	168.0	6.99
8.84	4.21	206.0	10.56	$\rho_{00}=4.15 \text{ g/cm}^3$; $m=2.12$			
10.52	5.20	303.0	10.94	1.21	0.615	3.1	8.43
$\rho_{00}=4.15 \text{ g/cm}^3$; $m=2.12$				4.14	2.21	38.0	8.90
1.96	1.02	8.3	8.64	5.27	2.82	61.7	8.93
2.65	1.40	15.4	8.80	6.30	3.31	86.5	8.75
3.24	1.71	23.0	8.79	6.78	3.63	102.0	8.91
Iron; $\rho_0=7.85 \text{ g/cm}^3$							
$\rho_{00}=4.3 \text{ g/cm}^3$; $m=1.826$				$\rho_{00}=2.706 \text{ g/cm}^3$; $m=2.9$			
1.434	0.598	3.7	7.38	1.092	0.646	1.9	6.63
2.19	0.974	9.2	7.74	1.87	1.16	5.9	7.12
2.87	1.335	16.5	8.03	2.54	1.61	11.1	7.39
3.55	1.635	24.9	7.99	3.15	1.98	16.9	7.29
5.55	2.71	65.6	8.52	5.38	3.27	47.6	6.90
6.32	3.14	85.1	8.55	6.46	3.84	67.1	6.67
6.48	3.22	89.7	8.55	7.08	4.25	81.4	6.77
7.14	3.59	110.0	8.65	7.16	4.27	82.4	6.70
10.41	5.61	251.0	9.33				

TABLE V.

Chromium; $\rho_0=7.18 \text{ g/cm}^3$							
<i>D</i> , km/s	<i>U</i> , km/s	<i>P</i> , GPa	ρ , g/cm ³	<i>D</i> , km/s	<i>U</i> , km/s	<i>P</i> , GPa	ρ , g/cm ³
$\rho_{00}=4.224 \text{ g/cm}^3$; $m=1.7$				$\rho_{00}=3.26 \text{ g/cm}^3$; $m=2.2$			
0.94	0.31	1.2	6.30	1.188	0.631	2.4	6.95
1.52	0.60	3.8	6.94	1.97	1.09	7.0	7.30
2.25	0.97	9.2	7.42	2.68	1.51	13.2	7.46
3.06	1.32	17.1	7.43	3.27	1.85	19.7	7.51
3.73	1.61	25.4	7.43	4.27	2.40	33.4	7.40
4.70	2.09	41.5	7.61	4.72	2.63	40.4	7.36
5.38	2.40	54.5	7.63	5.44	3.05	54.1	7.42
5.84	2.69	66.3	7.83	5.80	3.26	61.6	7.44
6.16	2.88	74.9	7.93	6.45	3.60	75.7	7.38
6.67	3.21	90.4	8.14	7.10	3.98	92.1	7.42
7.35	3.54	110.0	8.15	7.68	4.31	108.0	7.43
10.78	5.56	253.0	8.72				
Tantalum; $\rho_0=16.38 \text{ g/cm}^3$							
$\rho_{00}=10.92 \text{ g/cm}^3$; $m=1.5$				$\rho_{00}=6.20 \text{ g/cm}^3$; $m=2.64$			
1.895	0.70	14.5	17.31	0.966	0.601	3.6	16.40
2.50	0.94	25.5	17.50	1.58	0.956	9.5	15.70
3.67	1.49	59.7	18.38	2.62	1.595	25.9	15.84
4.34	1.90	90.0	19.42	3.37	2.04	42.6	15.71
4.40	1.95	93.6	19.61	3.88	2.37	57.0	15.93
5.00	2.33	127.0	20.45				
5.41	2.61	155.0	21.10				
$\rho_{00}=8.19 \text{ g/cm}^3$; $m=2.0$				$\rho_{00}=5.41 \text{ g/cm}^3$; $m=3.03$			
2.20	1.15	20.8	17.16	3.35	2.17	39.3	15.36
2.68	1.40	30.7	17.15	4.33	2.74	64.2	14.73
3.43	1.80	50.3	17.34	5.11	3.23	89.3	14.70
4.02	2.16	70.9	17.70				
4.27	2.30	80.4	17.75				
4.51	2.46	90.2	18.02				
4.97	2.71	111.0	18.09				
5.39	3.03	134.0	18.71				
				$\rho_{00}=2.82 \text{ g/cm}^3$; $m=5.81$			
				0.892	0.654	1.6	10.57
				1.531	1.20	5.1	13.07
				2.15	1.66	10.1	12.37
				2.66	2.06	15.4	12.50
				4.57	3.39	43.7	10.97
				6.10	4.43	76.2	10.30

TABLE VI.

Lead; $\rho_0=11.34 \text{ g/cm}^3$							
<i>D</i> , km/s	<i>U</i> , km/s	<i>P</i> , GPa	ρ , g/cm ³	<i>D</i> , km/s	<i>U</i> , km/s	<i>P</i> , GPa	ρ , g/cm ³
$\rho_{00}=9.51 \text{ g/cm}^3$; $m=1.19$				$\rho_{00}=6.79 \text{ g/cm}^3$; $m=1.67$			
2.03	0.46	8.9	12.30	1.51	0.55	5.6	10.66
2.46	0.66	15.4	12.98	2.01	0.85	11.6	11.75
3.35	1.16	37.0	14.56	2.58	1.17	20.4	12.42
4.65	2.04	90.1	16.94	3.04	1.44	29.7	12.90
5.73	2.73	149.0	18.16	4.53	2.44	75.0	14.72
				5.67	3.24	125.0	15.34
				7.81	4.85	257.0	17.91
$\rho_{00}=8.40 \text{ g/cm}^3$; $m=1.35$				$\rho_{00}=4.71 \text{ g/cm}^3$; $m=2.41$			
1.27	0.26	2.8	10.58	1.17	0.607	3.3	9.78
1.74	0.51	7.5	11.89	1.754	1.016	8.4	11.19
2.26	0.73	13.9	12.41	2.90	1.70	23.2	11.41
2.78	1.02	23.8	13.27	3.69	2.21	38.3	11.74
3.22	1.27	34.2	13.84	4.16	2.50	49.0	11.80
3.87	1.68	54.6	14.84	4.62	2.83	61.5	12.15
4.37	2.08	73.7	16.03	5.92	3.72	104.0	12.67
4.64	2.18	84.8	15.81	8.66	5.77	235.0	14.10
4.89	2.33	95.9	16.04				
5.27	2.61	115.0	16.64				
5.70	2.93	140.0	17.30				
8.24	4.91	340.0	20.79				
Magnesium; $\rho_0=1.74 \text{ g/cm}^3$							
$\rho_{00}=0.83 \text{ g/cm}^3$; $m=2.1$							
1.33	0.68	0.76	1.68	7.07	4.13	24.2	1.99
3.64	1.89	6.0	1.80	8.30	4.93	33.9	2.04
4.39	2.40	8.7	1.83	9.18	5.50	41.9	2.07
5.54	3.14	14.4	1.92				

TABLE VII.

Nickel; $\rho_0=8.87 \text{ g/cm}^3$							
D. km/s	U. km/s	P. GPa	$\rho. \text{ g/cm}^3$	D. km/s	U. km/s	P. GPa	$\rho. \text{ g/cm}^3$
$\rho_{00}=6.28 \text{ g/cm}^3; m=1.41$				$\rho_{00}=3.28 \text{ g/cm}^3; m=2.7$			
1.73	0.54	5.9	9.13	2.54	1.53	13	8.25
2.04	0.64	8.2	9.15	3.12	1.88	19	8.25
2.46	0.80	12	9.31	4.02	2.45	32	8.40
2.59	0.82	13	9.19	5.24	3.09	53	7.99
3.33	1.075	22	9.27	5.94	3.56	69	8.19
3.80	1.35	32	9.74	6.83	4.045	91	8.04
4.70	1.75	52	10.00				
5.75	2.26	82	10.35	$\rho_{00}=1.95 \text{ g/cm}^3; m=4.55$			
6.90	2.87	124	10.75	0.89	0.67	1.2	7.89
7.10	3.02	135	10.93	1.04	0.81	1.6	8.82
7.54	3.28	135	11.12	1.62	1.27	4.0	9.02
				2.34	1.77	8.1	8.08
$\rho_{00}=5.17 \text{ g/cm}^3; m=1.72$				2.99	2.19	13	7.29
2.98	1.23	19	8.80	3.88	2.86	22	7.42
4.39	1.98	45	9.42	5.14	3.64	36	6.68
5.53	2.52	72	9.50	5.60	3.95	43	6.62
6.39	3.12	103	10.10	6.94	4.76	64	6.21
6.84	3.36	119	10.16	7.58	5.12	76	6.01
7.35	3.63	138	10.21				
$\rho_{00}=4.43 \text{ g/cm}^3; m=2.0$				$\rho_{00}=1.59 \text{ g/cm}^3; m=5.58$			
1.25	0.61	3.4	8.65	0.86	0.67	0.9	7.20
1.42	0.73	4.6	9.12	1.02	0.82	1.3	8.11
2.70	1.36	16	8.93	1.60	1.31	3.3	8.77
3.28	1.665	24	9.00	2.34	1.84	6.8	7.44
4.26	2.12	40	8.82	3.03	2.28	11	6.42
5.30	2.74	64	9.17	3.90	3.00	19	6.89
6.24	3.25	90	9.24	5.20	3.83	32	6.04
6.90	3.58	109	9.21	5.63	4.06	36	5.70
7.39	3.86	126	9.27	6.07	4.56	44	6.39
				7.00	5.02	56	5.62
				7.42	5.44	64	5.96
$\rho_{00}=3.85 \text{ g/cm}^3; m=2.30$				$\rho_{00}=1.23 \text{ g/cm}^3; m=7.21$			
2.56	1.45	14	8.88	2.37	1.91	5.6	6.34
3.18	1.77	22	8.68	3.03	2.39	8.9	5.82
4.07	2.23	36	8.80	3.97	3.15	15	5.95
5.26	2.81	59	8.60	5.30	4.04	26	5.17
6.08	3.41	80	8.77	7.07	5.31	46	4.94
6.83	3.81	100	8.70	7.70	5.73	54	4.81
$\rho_{00}=1.65 \text{ g/cm}^3; m=5.38$							
3.89	2.97	19	6.98	7.13	4.96	58	5.42
5.26	3.79	33	5.90	7.55	5.36	67	5.69

TABLE VIII.

Tungsten; $\rho_0=19.17 \text{ g/cm}^3$							
D. km/s	U. km/s	P. GPa	$\rho. \text{ g/cm}^3$	D. km/s	U. km/s	P. GPa	$\rho. \text{ g/cm}^3$
$\rho_{00}=13.36 \text{ g/cm}^3; m=1.43$				$\rho_{00}=8.87 \text{ g/cm}^3; m=2.16$			
2.53	0.84	28	20.00	1.07	0.56	5.3	18.61
3.61	1.35	65	21.34	2.12	1.13	21	18.99
4.39	1.74	102	22.13	3.25	1.77	51	19.48
4.41	1.74	102	22.07	4.13	2.24	82	19.38
5.49	2.31	169	23.06	5.24	2.95	137	20.30
5.87	2.54	199	23.55	5.68	3.17	160	20.07
$\rho_{00}=6.64 \text{ g/cm}^3; m=2.89$				$\rho_{00}=5.50 \text{ g/cm}^3; m=3.48$			
2.04	1.295	17	18.18	2.06	1.38	16	16.66
3.21	2.03	48	18.06	3.25	2.18	39	16.70
3.71	2.35	58	18.11	3.71	2.47	50	16.45
4.08	2.68	70	18.06	4.20	2.76	64	16.04
5.32	3.355	118	17.98	5.40	3.63	108	16.78
5.83	3.60	139	17.36	6.00	3.86	127	15.42
6.01	3.685	147	17.16	6.05	3.885	129	15.37
$\rho_{00}=4.60 \text{ g/cm}^3; m=4.17$							
2.14	1.45	14	14.27	5.17	3.44	82	13.75
3.30	2.32	35	15.49	5.55	3.85	98	15.02
3.70	2.57	44	15.06	6.08	4.07	114	13.91
4.26	2.94	58	14.84	6.20	4.095	117	13.55

TABLE IX. Data for nickel from Ref. 1, reduced by A. I. Funtikov by a procedure similar to that of Ref. 7.

m	ρ_{00} , g/cm ³	D , km/s	U , km/s	P , GPa	ρ , g/cm ³
1.0	8.9	14.89	7.36	976	17.60
1.43	6.22	9.74	4.62	280	11.83
1.75	5.09	9.42	5.01	240	10.87
	5.09	15.67	8.91	711	11.80
3.0	2.97	9.21	5.78	158	7.97
	2.97	15.93	10.31	488	8.42

ing slopes of the adiabats with $m = 1$. After rectification, the adiabats in the $D-U$ plane are parallel. The maximum adiabat slope is known^{1,2} to be $D'_u \approx 1.2$.

We proceed now to the experimental data plotted in the $P-\rho$ plane (Figs. 5 and 6). We must consider here, first of all, the question of the so-called "packing pressures" P_{pp} . These are taken to mean the pressures on the considered adiabat of the porous metal (for $m > 1$) corresponding to a certain limiting point (P_{pp}) through which the adiabats are extrapolated to the initial state ($P = 0$; $\rho = \rho_{0,cr}$). The very postulation of packing pressures implies that shock adiabats corresponding to decreased density do not reach the density of the solid metal at the point $P = 0$, $\rho_0 = \rho_{0,cr}$, and that a state with these parameters is not a common point of a family of adiabats of different initial density. This has been demonstrated, in particular, in Ref. 4 and is confirmed by our experimental data.

It follows from an examination of the $P-\rho$ diagrams that shock adiabats of porous metals (with $m > 1.5-2.0$) consist of two main sections—the first (up to the packing pressures) gently sloping and the second steep. Extrapolation of the second sections of the adiabats to zero pressures (through the point P_{pp}) corresponds to the corresponding crystallographic densities $\rho_{0,cr}$.

For the metals investigated in wide ranges of m [i.e., for Cu, Mo, Ni, and Ta), the adiabats centered to $\rho_{0,cr}$ are characterized by different slope $(dP/d\rho)_\Gamma$, both positive and negative, including vertical adiabats ($(dP/d\rho)_\Gamma = \infty$].

It is known^{1,2} that at large m , in view of their strong heating by the shock waves, the samples can have states in which an increase of the amplitude of the shock wave acting on the sample decreases rather than increases its density. We obtained such states for $m = 7.2, 7.2$, and 8.0 in copper,

nickel, and molybdenum, respectively. The largest "under-compressions" were obtained in copper, with $\rho = 0.55 \rho_{0,cr} = 4.95 \text{ g/cm}^3$ ($P \approx 47 \text{ GPa}$) for $m = 7.2$. The shock-compression energy is in this case $E_\Gamma \approx 14.0 \text{ kJ/g}$. Such values of E_Γ on the adiabat of "solid" copper are reached for $P_\Gamma \approx 560 \text{ GPa}$, when the samples are compressed by the shock wave to $\rho \approx 1.8 \rho_{0,cr}$. What is the role of heat in these states? With allowance for the cold energy E_c of the elastic interaction of the atom (estimates give $E_c \approx 1.5 \text{ kJ/g}$), the thermal energy on the adiabat of porous copper ($m = 7.2$) at $P_\Gamma \approx 47 \text{ GPa}$ is $E_t = E_\Gamma - E_c \approx 12.5 \text{ kJ/g}$, i.e., practically all the shock-compression energy is thermal. Estimates yield for the pressure components $P_c = -19 \text{ GPa}$ and $P_h \approx 66 \text{ GPa}$. The picture is different on the shock adiabat of solid copper ($m = 1$). For $P_\Gamma \approx 560 \text{ GPa}$ we obtain $P_c \approx 360 \text{ GPa}$ and $P_h \approx 200 \text{ GPa}$. Accordingly $E_h \approx 9.0 \text{ kJ/g}$ ($E_c \approx 5.0 \text{ kJ/g}$; $E_\Gamma \approx 4.0 \text{ kJ/g}$). It can be seen that in this case elastic interaction of the atoms play a rather weighty role. Similar relations are obtained also for adiabats of other metals at low initial density. Thus, for molybdenum ($\rho_{00} = 1.277 \text{ g/cm}^3$) at $\rho = 6.44 \text{ g/cm}^3$ we have $P_h \approx 26 \text{ GPa}$; $E_\Gamma \approx 8.0 \text{ kJ/g}$, $E_h \approx 6.0 \text{ kJ/g}$, $P_c \approx -48 \text{ GPa}$, and $P_h \approx 74 \text{ GPa}$. The same shock-compression energy is reached on the adiabat of solid molybdenum at $P_\Gamma \approx 420 \text{ GPa}$; in this case $E_c \approx 5.0 \text{ kJ/g}$, $E_h \approx 3.0 \text{ kJ/g}$, $P_c \approx 370 \text{ GPa}$, and $P_h \approx 50 \text{ GPa}$.

It follows from general considerations that the slopes $(dP/d\rho)_\Gamma$ of shock adiabats of samples having high porosity ($m \geq 2$) reverse sign as the pressure is increased. The cause is the progressive increase of the fraction of kinetic energy in the total energy compared with the potential fraction—an ideal gas in the limit of high temperatures (maximum value $\rho_\Gamma = 4\rho_{00}$). This law holds for a number of the metals investigated here in the experimental range of states

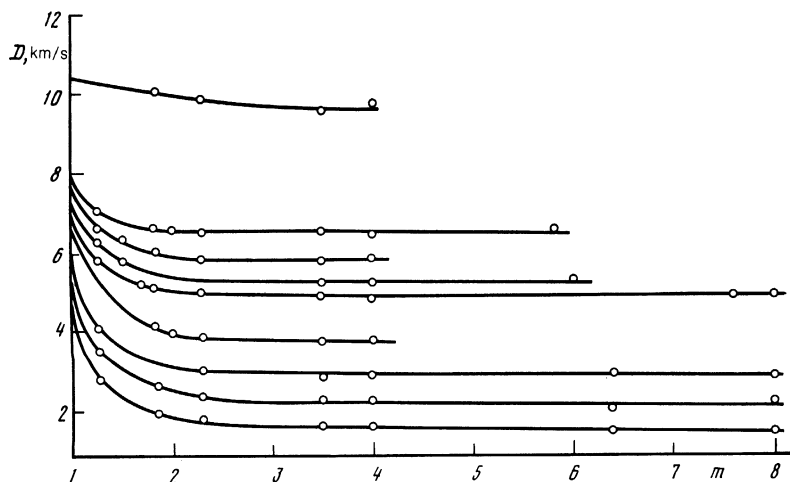


FIG. 1. Plot of $D(m)$ obtained for molybdenum in the present study. Each curve corresponds to a specific measurement setup, i.e., to specific shock-wave parameters in the screen and in the investigated samples.

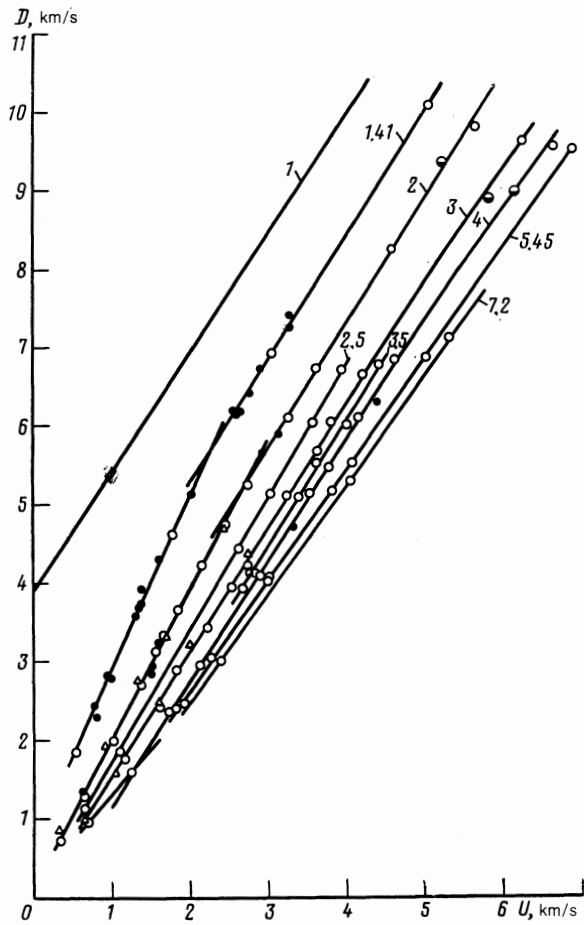


FIG. 2. $D-U$ diagram for copper: \circ —our data; \bullet , \blacktriangle , and \ominus —data of Refs. 5, 4, and 7, respectively.

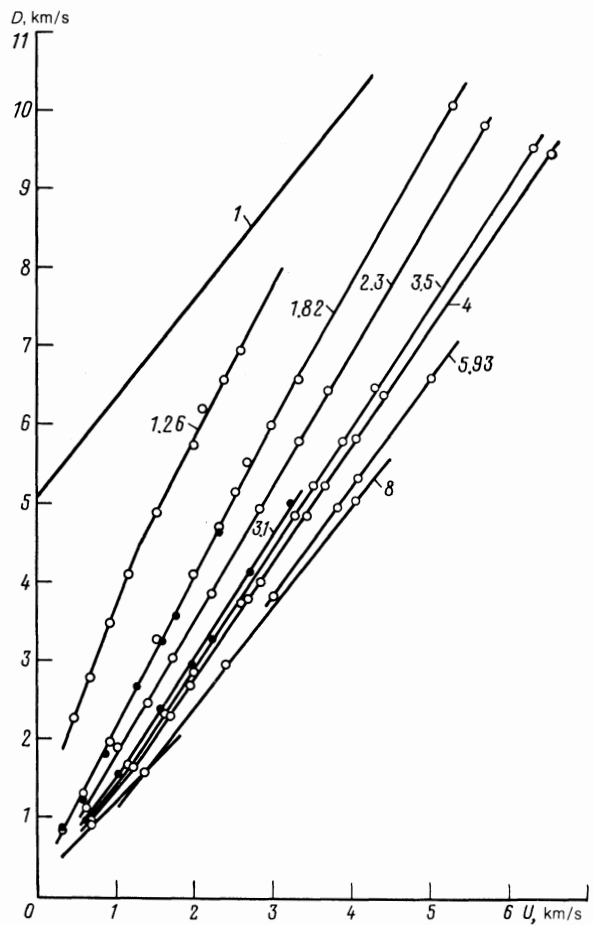


FIG. 4. $D-U$ diagram for molybdenum: \circ —our data, \bullet —from Ref. 4.

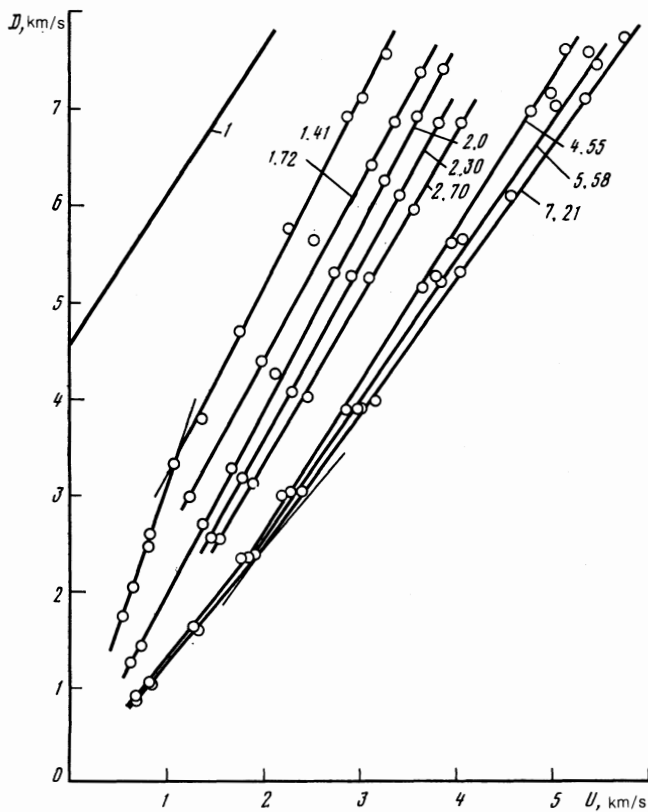


FIG. 3. $D-U$ diagram for nickel; our data.

[e.g., copper (Fig. 5), tantalum, and iron]. For other metals [e.g., molybdenum (Fig. 6)] no sign reversal of $(dP/d\rho)_r$ is observed in the investigated region; a sign reversal should be expected at higher pressures.

The relative positions of the experimental adiabats, the different signs of the slopes P'_ρ for the considered metal, and the range of the densities investigated by us are such that the simple and frequently employed equations, for example those in which the thermal pressures and the energy are connected by the average Grüneisen coefficient $\bar{\Gamma} = \text{const}$ or by $\Gamma(v)$, are of little use already because of the shapes of the shock adiabats.

A better description of the experiment is obtained by using the equation of state of Ref. 8, in the form

$$E - E_r = \frac{P_r}{\eta(P)} (V - V_r) \quad (1)$$

with a proportionality coefficient $\eta(P) = P(\partial V / \partial E)_P$. For certain metals (Pb, W, Ni), however, a comparison of the shock adiabats leads to a more complicated multiparameter dependence of the coefficient η . This is naturally manifested also in the accuracy of the experimental data. We have chosen therefore a more general approach, without determining the empirical coefficients in the equations by using all experimental data on the shock compressibility, even though this leads to a somewhat poorer agreement with the description of the maximum-porosity adiabats by Eq. (1).

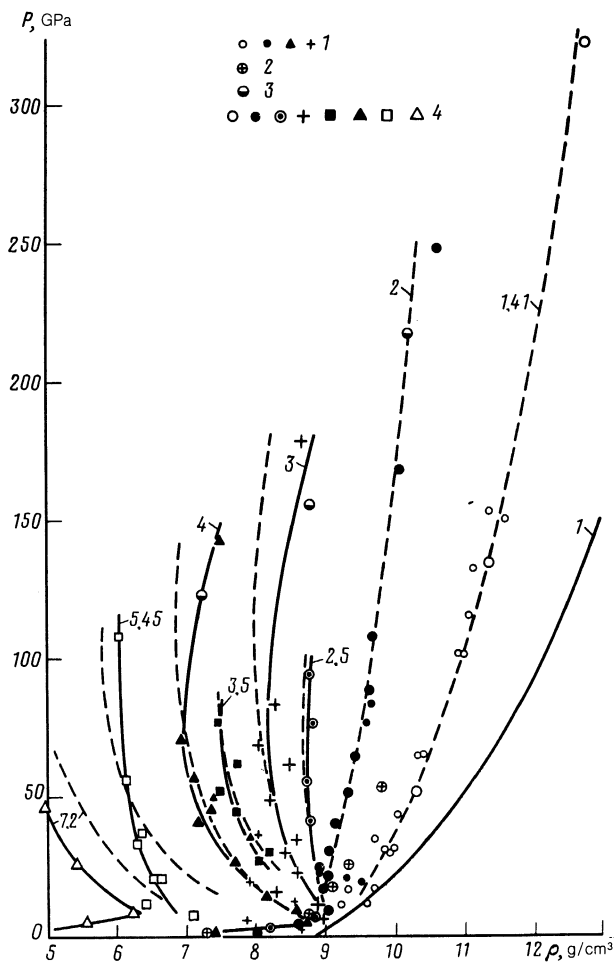


FIG. 5. Plots of P vs ρ for copper with different porosities; 1—Ref. 5, 2—Ref. 4, 3—Ref. 7, 4—present data; solid lines—experiment, dashed—calculation.

The equation of state was specified in a form similar to that used in Ref. 7:

$$P = P_r + \xi_r (V - V_r), \quad (2)$$

$$PV = P_r V_r + \frac{2}{3} (E - E_r). \quad (3)$$

The index “ Γ ” pertains to the solid-material ($m = 1$) shock adiabat used as the reference curve. An equation of state in the form (2), (3) is an expansion of the product PV in a series of terms of first-order in energy. The expansion is along the connecting lines (2), which constitute a single-parameter family of straight P vs V plots; the parameter is some characteristic on the shock adiabat $m = 1$ (for example, V_r), with which the others (P_r, E_r, ξ_r) are assumed to be uniquely connected. The slope $\xi (\equiv dP/dV)$ of the connecting lines is obtained from the condition that the following equality hold near the reference curve (“ Γ ”):

$$\frac{\partial(PV)}{\partial E} = \frac{2}{3}. \quad (4)$$

The differentials of the numerator and denominator in (4) are equal to

$$d(PV) = P dV + V dP, \quad (5)$$

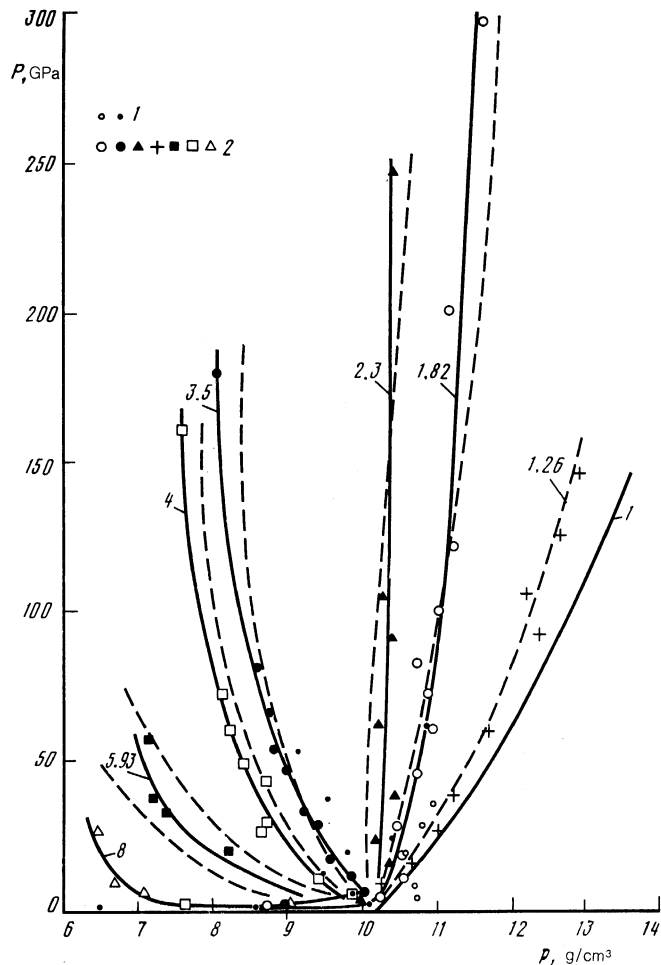


FIG. 6. Dependences of P on ρ for molybdenum at various porosities; 1—Ref. 4, 2—present data; points and solid lines—experiment, dashed lines—calculation.

$$dE = \left(\frac{\partial E}{\partial V} \right)_P dV + \left(\frac{\partial E}{\partial P} \right)_V dP. \quad (6)$$

The derivative $(\partial E / \partial P)_V$ is expressed in terms of the Grüneisen coefficient Γ and the density ρ as follows:

$$\left(\frac{\partial E}{\partial P} \right)_V = \frac{1}{\Gamma \rho}. \quad (7)$$

After some transformations, $(\partial E / \partial V)_P$ can be written in the form:

$$\left(\frac{\partial E}{\partial V} \right)_P = \frac{\rho c^2}{\Gamma} - P, \quad (8)$$

where c is the speed of sound.

Substitution of (5) and (6) in (4), with allowance for (7) and (8), yields

$$\left(P + \frac{1}{\rho} \frac{dP}{dV} \right) / \left[\left(\frac{\rho c^2}{\Gamma} - P \right) + \frac{dP}{\Gamma \rho dV} \right] = \frac{2}{3}. \quad (9)$$

From this we get

$$\xi_r = (\rho_r c_r)^2 \left(\frac{2}{3} - \frac{5}{3} \frac{\Gamma_r P_r}{\rho_r c_r^2} \right) / (\Gamma_r^{-2/3}). \quad (10)$$

Since this expression was obtained from (4), the expansion of PV in terms of E along the straight lines (2) yields Eq.

(3). For simplicity, we assume here that ξ_r is constant on the reference curve ($m = 1$):

$$\xi_r = \frac{2}{3} \frac{(\rho_0 c_0)^2}{\Gamma_0^{-2/3}}, \quad (11)$$

and use the subscript "0" to label quantities under normal conditions. Note that in the limit as $V \rightarrow \infty$ the equation of state in the form (2), (3) becomes the equation of state $PV = \frac{2}{3}E$ of an ideal monatomic gas under the condition $\xi_r > 0$. Since the value of Γ_0 in (11) for metals is ≈ 2 , it follows that $\xi_r > 0$. The shock adiabats of the solid metals, needed to obtain an equation of state in this form, were taken from Ref. 9. For the experimental data on porous metal samples we used for Γ_0 in (11) the following values: Cu—1.6; Co—2.3; Mo—1.8; Fe—2.0; Pb—2.5; Cr—1.3; Ta—1.7; Mg—1.0; Ni—2.2; W—1.8. They are close, but not always exactly equal, to those given for example in Ref. 10. The chosen values of Γ_0 provide a better description of the experimental results. Some differences between the assumed Γ_0 and the Gruneisen coefficients given in Ref. 10 may be due to the fact that in most cases the investigated porous metals behind the shock-wave are certainly in a liquid state, where Γ_0 can differ from the solid-state Γ_0 . The shock adiabats of the porous substances were calculated by solving (2) simultaneously with Eq. (3) transformed, by using the connection between E , P , and V under shock compression, to the following form:

$$PV - P_r V_r = \frac{P(V_0 - V) - P_r(V_0 - V_r)}{3}. \quad (12)$$

By way of illustration, Figs. 5 and 6 show the calculated shock adiabats of copper and molybdenum with various porosities. On the whole, the experimental data are not badly described. Significant deviations are observed only for the maximum values of the porosity. A similar picture is obtained also for all other metals.

A few concluding remarks concerning the accuracy with which the compression ($\sigma = \rho/\rho_0$) was calculated for the adiabats of porous samples. The error is equal to

$$\Delta\sigma = \sigma(m\sigma - 1)(|\Delta U/U| + |\Delta D/D|).$$

The accuracy of the recorded kinematic parameters D and U is estimated at $\sim (1-2)\%$, while the error $\Delta\sigma$ increases with σ and m . Formally, the error for large m becomes quite substantial, even though the error of the compressibility determined in this case is partially cancelled by the transition to the region of states corresponding to $\sigma < 1$. Judging, however, from the mutual consistency of numerous data obtained for many adiabats of metals with different porosities and in large ranges of P - ρ states, the most probable experimental values of σ have been determined reliably enough.

The most sensitive to errors of D and U are measurements at low pressures. The errors of the adiabats measured in this region ($P_r < 3$ GPa) are therefore too large to speak of an accurate quantitative determination. The situation is improved somewhat when aggregates of results for many values of m of the metal in question are considered.

¹The data of Ref. 1 were reduced by A. S. Funtikov.

²The porosity of the sample is marked on each adiabat; $m = 1$ for solid substances.

³S. B. Kormer, A. I. Funtikov, V. D. Urlin, and A. I. Kolesnikova, Zh. Eksp. Teor. Fiz. **42**, 686 (1962) [Sov. Phys. JETP **15**, 477 (1962)].

⁴K. K. Krupnikov, M. I. Brazhnik, and V. P. Krupnikova, *ibid.* p. 675 [470].

⁵V. N. Zubarev, M. A. Podurets, L. V. Popov, G. V. Simakov, and R. F. Trunin, in: *Detonation. Critical Phenomena. Physico-Chemical Transformations in Shock Waves*. Publ. by Inst. of Chem. Phys., USSR Acad. Sci., 1978.

⁶A. A. Bakanova, I. P. Dudoladov, and Yu. N. Sutulov, Prikl. Mat. Tekh. Fiz. No. 2, 117 (1974).

⁷R. G. McQueen, S. P. March, T. Taylor, and W. J. Carter, *High-Speed Shock Phenomena* [Russ. transl.], Mir, 1973.

⁸L. V. Al'tshuler, K. K. Krupnikov, and M. I. Brazhnik, Zh. Eksp. Teor. Fiz. **34**, 686 (1958) [Sov. Phys. JETP **7**, 614 (1958)].

⁹R. F. Trunin, A. B. Medvedev, A. I. Funtikov, M. A. Podurets, G. V. Simakov, and A. G. Sevast'yanov, Zh. Eksp. Teor. Fiz. **95**, 631 (1989) [Sov. Phys. JETP **68**, 356 (1989)].

¹⁰A. A. Bakanova, V. N. Zubarev, Yu. N. Sutulov, and R. F. Trunin, *ibid.* **68**, 1099 (1975) [41, 544 (1975)].

¹¹L. V. Al'tshuler, A. A. Bakanova, I. P. Dudoladov, E. A. Dynin, R. F. Trunin, and B. S. Chekin, Prikl. Mat. Tekh. Fiz. No. 2, 3 (1981).

Translated by J. G. Adashko